How Semiphysiological Population Pharmacokinetic Modeling Incorporating Active Hepatic Uptake Supports Phase II Dose Selection of RO7049389, A Novel Anti–Hepatitis B Virus Drug

Valérie Cosson[1,*], Sheng Feng[2], Felix Jaminion[1], Annabelle Lemenuel-Diot[1], Neil Parrott[1], Axel Paehler[1], Qingyan Bo[3] and Yuyan Jin[2]

The pharmacokinetics (PK) of RO7049389, a new hepatitis B virus (HBV) core protein allosteric modulator of class I, and of its active metabolite M5 were studied in fasted and fed conditions after single and multiple once-a-day and twice-a-day doses in healthy subjects and patients with HBV. The nonlinearity of the pharmacokinetics, the large variability, the small sample size per dose arms, the higher plasma exposure in Asians, and the heterogeneity in patient baseline characteristics seen in phase I studies made the ethnic sensitivity assessment and the selection of the recommended phase II dose difficult. A population PK model, simultaneously modeling RO7049389 and M5, was developed to characterize the complex PK, quantify ethnicity (i.e., Asian vs. non-Asian) and gender effects on the PK of RO7049389 and M5, and infer the quantity of RO7049389 in liver relative to plasma. Exposures in the liver are of particular importance for dose selection since the liver is the site of action of the compound. The model described and reproduced the population PK profiles as well as the between-subject variability of RO7049389 and its metabolite. It could show that the PK is similar between healthy subjects and in HBV patients, once the ethnicity and gender effects are accounted for. The model predicts that, despite a large difference in the plasma exposure of RO7049389 between Asians and non-Asians, the exposure in the liver is comparable, allowing the use of the same dose to treat Asian and non-Asian patients. This model provides a valuable basis to develop this new anti-HBV drug and to define optimal dosing.

Study Highlights

WHAT IS THE CURRENT KNOWLEDGE ON THE TOPIC?

☑ Core protein allosteric modulators like RO7049389, a novel class of drugs targeting the hepatitis B virus (HBV) capsid assembly, are under development to treat HBV infection. The population pharmacokinetics (PK) of RO7049389 has not been reported yet.

WHAT QUESTION DID THIS STUDY ADDRESS?

☑ The analysis described here aimed to support the selection of the phase II dose by the characterization of the PK in plasma of RO7049389 and its metabolite M5, the quantification of the amount of RO7049389 in the liver, and the assessment of the impact of ethnicity on the PK of both parent and metabolite.

WHAT DOES THIS STUDY ADD TO OUR KNOWLEDGE?

☑ This model provides the first PK characterization of RO7049389 in plasma and the liver, and it shows that, despite a large difference in the plasma exposure of RO7049389 between Asians and non-Asians, its estimated exposure in the liver (the site of action) is similar.

HOW MIGHT THIS CHANGE CLINICAL PHARMACOLOGY OR TRANSLATIONAL SCIENCE?

☑ The model will be used for exposure–response analyses to evaluate and predict relevant clinical outcomes in the phase II trial. In addition, these findings may inform PK analyses of other compounds undergoing active uptake by organic anion transporting polypeptide 1B (OATP1B) transporters.

[1]Pharmaceutical Sciences, Roche Pharma Research & Early Development, Roche Innovation Center Basel, Basel, Switzerland; [2]Pharmaceutical Sciences, Roche Pharma Research & Early Development, Roche Innovation Center Shanghai, Shanghai, China; [3]Immunology, Infectious Diseases and Ophthalmology Discovery and Translational Area, Roche Pharma Research & Early Development, Roche Innovation Center Shanghai, Shanghai, China. *Correspondence: Valérie Cosson (valerie.cosson@roche.com)

Received November 5, 2020; accepted January 16, 2021. doi:10.1002/cpt.2184

INTRODUCTION

Hepatitis B virus (HBV) infects liver cells and can cause both acute hepatitis and chronic liver diseases, which may lead to cirrhosis, liver failure, and hepatocellular carcinoma. Approximately 257 million people worldwide are living with chronic hepatitis B (CHB) infection. In 2015, HBV infection resulted in an estimated 887,000 deaths, mostly from complications including cirrhosis and hepatocellular carcinoma.[1,2]

Currently, there are two classes of drugs available for treatment of CHB: subcutaneously administered interferon alpha and orally administered nucleos(t)ide analogs. Interferons are indicated for long-term immune control by finite treatment while nucleos(t)ide analog long-term treatments result in an HBV DNA suppression effect. Neither treatment achieves a high rate of functional cure defined as hepatitis B surface antigen (HBsAg) loss.

RO7049389, a small molecule developed as an orally administered solid dosage formulation, is a class I core protein allosteric modulator that induces the formation of abnormal HBV core protein aggregates, leading to depletion of functional core protein and defective capsid structure assembly, resulting in suppression of viral replication.[3,4,5]

Up to April 2019, RO7049389 or placebo was administered orally in both healthy volunteers (HVs) and HBV patients (different doses, up to 28 days) in three phase I studies. The data showed good safety and efficacy supporting further development in phase II. RO7049389 is rapidly absorbed and eliminated from plasma without accumulation after b.i.d. or q.d. multiple dosing.[6] Three metabolites of RO7049389 that exceed 10% of total drug-related material in human plasma were identified, among which M5, the only active metabolite, exceeds exposure of RO7049389. Greater-than-dose-proportional increases in RO7049389 plasma exposure and less-than-dose-proportional increases in metabolite plasma exposure were observed.[6] The plasma exposure of RO7049389 in Asian HVs was much higher than that in non-Asian HVs.

The elimination of RO7049389 appears to be mainly mediated by liver metabolism (oxidation via cytochrome P450 (CYP) 3A4 as the major route and direct glucuronidation via uridine 5′-diphospho glucuronosyltransferase (UGT) 1A3 as a minor route); however, a contribution of biliary clearance cannot be excluded. Furthermore, RO7049389 is a substrate of human liver uptake transporters, organic anion transporting polypeptide 1B1 (OATP1B1) and OATP1B3 and, as a result, shows strong accumulation in hepatocytes (results from *in vitro* studies; data not shown). RO7049389 has moderate passive permeability and is a substrate of human P-glycoprotein (Pgp) but not for the breast cancer resistance protein (BCRP) transporter.

The nonlinearity of the pharmacokinetics (PK), the large PK variability, the small sample size per dose arms, the higher plasma exposure in Asians, and the heterogeneity in patient baseline characteristics seen in phase I studies made the ethnic sensitivity assessment and the selection of the recommended phase II dose difficult.

Here, we describe a population pharmacokinetic (popPK) analysis of RO7049389 and its active metabolite M5 performed on pooled data from three phase I studies. This novel analysis allowed for the description of the pharmacokinetics of RO7049389 and M5 in HVs and HBV patients. It can particularly describe the nonlinearity as well as the impact of ethnicity effect observed on the parent and metabolite PK. As the liver is the site of action of RO7049389, the ability of the model to infer RO7049389 exposures in the liver is of particular importance for dose selection. Moreover, such popPK modeling allows evaluating potential PK differences between different types of subjects (i.e., HVs and HBV patients), as well as quantifying the between-subject variability, and identifying additional covariates that may explain part of this variability.

METHODS

Subjects and trial design

The following three studies were conducted in accordance with Good Clinical Practice guidelines and the Helsinki Declaration of 1975 (as revised in 1983). All subjects provided written informed consent, and the protocols were approved by independent ethics committees.

The first-in-human, global phase I/II, multicenter study (NCT02952924) of RO7049389 consisted of three parts. Parts 1 and 2 detailed below were randomized, double-blinded, and placebo-controlled. Part 3, a nonrandomized, noncontrolled, open-label part evaluating the antiviral effect of RO7049389 on top of standard of care over 48 weeks in CHB patients, is currently ongoing and data are not accounted here.

Part 1 investigated the safety, tolerability, and pharmacokinetics of RO7049389 in 83 HVs. Among them, 41 received a single dose of RO7049389 or placebo in six cohorts (150, 450, 1,000 (repeated twice), 2,000 or 2,500 mg), and 42 received repeated b.i.d. doses of RO7049389 or placebo for 14 days (except for 800 mg dosed only for 3 days) in five cohorts (200 mg fasted or with standard meal, and 400, 600, or 800 mg with standard meal). Part 2 evaluated the safety, tolerability, pharmacokinetics, and efficacy of orally administered RO7049389 in CHB patients as proof of mechanism. Thirty-seven patients were treated in five cohorts with the following doses: 200 or 400 mg b.i.d., 200, 600, or 1,000 mg q.d. of RO7049389 or matching placebo for 28 days; 35 patients completed the 4-week treatment period.

The single-center, randomized, sponsor-open, double-blinded, placebo-controlled, single ascending dose (SAD) and multiple ascending dose (MAD) study (NCT03570658) investigated single and multiple doses of RO7049389 in healthy subjects of Chinese descent for comparison with healthy subjects in part 1 of global phase I/II study (NCT02952924). In total, 28 HVs in three SAD cohorts (200, 400, or 600 mg of RO7049389 or matching placebo) and 24 HVs (of which, 21 also participated in the SAD cohorts) in two MAD cohorts (200 or 400 mg b.i.d. of RO7049389 or matching placebo) were treated and completed the study.

The open-label, fixed sequence, two-period study (NCT03717064) investigated the effect of RO7049389 on the pharmacokinetics of pitavastatin in HVs. In Period 1, a single dose of pitavastatin of 2 mg was administered. In Period 2, RO7049389 was administered at a dose of 800 mg b.i.d. for 6 days; on day 4 a single dose of pitavastatin 2 mg was administered. Periods 1 and 2 were separated by a washout period of 7 to 21 days. In total, 17 HVs were dosed and completed the study.

Sampling and analytical methods

In order to get rich PK profiles of RO7049389 and M5, plasma samples were collected in HVs after single and multiple doses as well as in HBV patients after multiple doses. In part 1 MAD of the global phase I/II study and in the Chinese phase I study, full PK profiles after the first and last doses (i.e., on days 1 and 14) and serial trough levels on several days were obtained. In part 2 (proof of mechanism), full PK profiles after the first and last doses (i.e., on days 1 and 28) and serial trough levels on several days were obtained. Finally, in period 2 of the pitavastatin interaction study, 12-hour PK profiles on days 3 and 4 were obtained, and only the data collected on day 3 (i.e., without

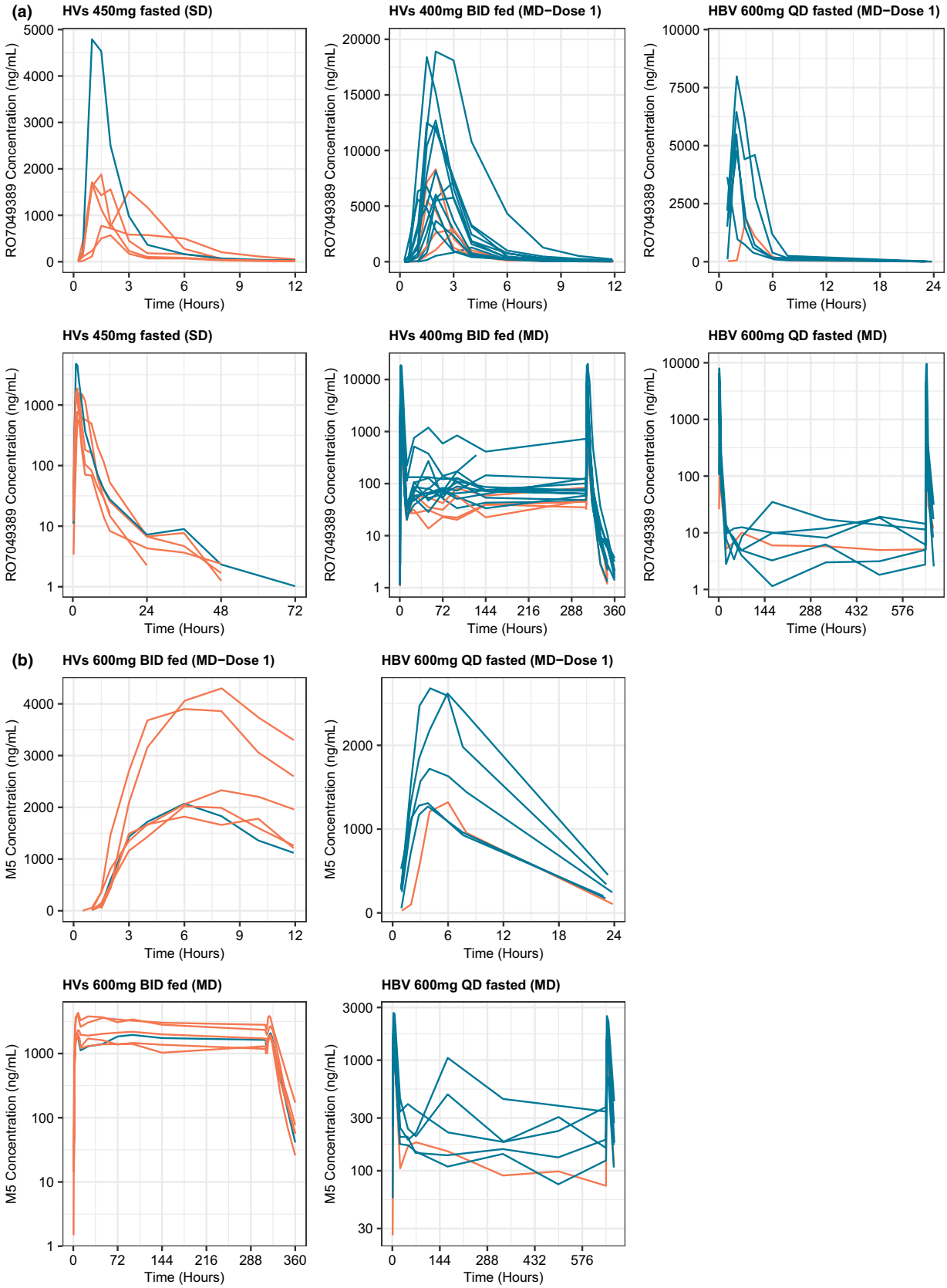

Figure 1 Pharmacokinetic profiles in healthy volunteers and patients with HBV colored by ethnicity group for (**a**) RO7049389 and (**b**) M5. Blue curves, PK profiles in Asians; Red curves, PK profiles in non-Asians. Upper row of each panel, linear Y scale, focus on the first 12 or 24 hours. Lower row of each panel, logarithmic Y scale, full profiles. b.i.d., twice a day; HVs, healthy volunteers; MD, multiple doses; PK, pharmacokinetic; SD, single dose; q.d., once a day.

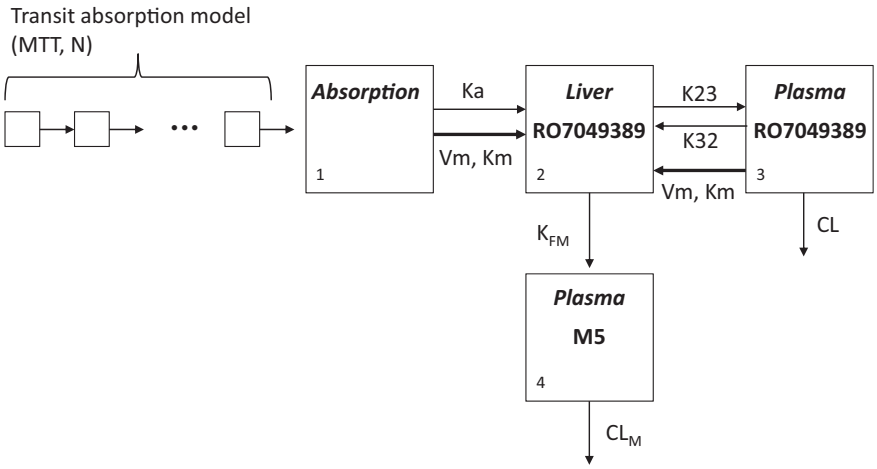

Figure 2 Schematic of the PK model. Plasma volume of M5 (V4) was assumed to equal plasma volume of RO7049389 (V3). CL, dose-dependent clearance of RO7049389 via non-M5 metabolic pathway and potential biliary secretion; CL_M, clearance of M5; Ka, the absorption rate constant (first order process); K_{FM}, M5-formation rate constant (first-order process); Km, Michaelis-Menten constant of the liver uptake capacity; K23 and K32, mass-transfer rate constants between liver and plasma compartments (first order processes); MTT, the mean transit time; N, number of transit compartments; PK, pharmacokinetic; Vm, maximum liver uptake capacity.

pitavastatin) were used to describe the PK of RO7049389 and M5. M5 PK assessments were introduced in the course of the global phase I/II study part 1 and performed only for the 2,500 mg single dose and the 600 mg b.i.d. multiple dose.

Plasma concentrations of RO7049389 and M5 were measured using specific and validated liquid chromatography-electrospray ionization-tandem mass spectrometry methods conducted in a Good Laboratory Practice compliance environment. The limit of quantification was 1.0 ng/mL, with a calibration range of 1.0 to 2,000 ng/mL for both RO7049389 and M5. More details on the assay method are provided in Supplementary Material.

PK modeling and simulations

A population PK model, simultaneously modeling RO7049389 and M5 and accounting for active and saturable liver uptake of RO7049389, was developed. This model was applied to infer the quantity of RO7049389 in the liver relative to plasma and to quantify the effect of ethnicity on the PK of RO7049389 and M5. Different structures were tested based on the PK properties of the drug. To describe the residual variability (RV), both proportional and a combination of additive and proportional RV were tested. The between-subject variability (BSV) in the model parameters was assumed to be log-normally distributed and was evaluated on all parameters. The need for eta correlations was also investigated.

The investigation of the effect of ethnicity, i.e., Asian vs. non-Asian, on the PK of RO7049389 and M5 was one of the main objectives of this analysis. Given that RO7049389 was administered in fasted and fed conditions, food effect was tested on the absorption and relative bioavailability parameters. The effects of body weight, age, gender, and patient type (i.e., HVs or HBV patients) on PK parameters were investigated. The covariate analysis started with a graphical exploration of the covariate effects on the etas of the parameters. Only the covariates leading to a change in standard deviation (SD) of ~ 1 or more were tested. Additional technical details on PK modeling are provided in Supplementary Material.

Simulations with the final model were performed to support the dose selection for phase II. To illustrate and quantify the impact of ethnicity on the exposure of RO7049389 in plasma and liver, and on the exposure of M5 in plasma, 500 time courses in male and female Asian and non-Asian subjects were simulated at different doses of RO7049389 (200, 400, 600, and 1,000 mg) administered q.d. in the fasted condition for 27 days. Individual exposure parameters at steady state, i.e., maximum plasma concentration (C_{max}), area under the plasma concentration profile (AUC), maximum liver amount (A_{max}), and area under the liver amount profile (AUQ), were derived and summarized by dose and relevant covariates.

RESULTS

Population PK analysis

The population PK data set consisted of 2,994 RO7049389 and 1,983 M5 plasma concentrations from 135 individuals (105 HVs and 30 HBV patients) treated with single and multiple doses of RO7049389. Overall (**Table S1**), 13% of the individuals were female (7% of HVs and 37% of patients) and 45% were Asian (33% of HVs and 87% of patients). At baseline, the analysis population had a median weight of 71.7 kg and a median age of 29 years.

The observed PK profiles of RO7049389 in HVs and in HBV patients exhibit a rapid elimination of the drug with low levels after 24 hours and no accumulation after multiple doses. The comparison of PK plots between Asian and non-Asian HVs show 2-to-3 times higher levels of RO7049389 in Asians as illustrated with sampled plots after single and multiple doses in **Figure 1**(**a**). As for the parent compound, the observed PK profiles of M5 display a rather rapid elimination of the metabolite and no accumulation after multiple doses (**Figure 1b**).

The structural model that best fitted simultaneously RO7049389 and metabolite M5 plasma concentrations in HVs and HBV patients (**Figure 2**) consists of (i) a liver compartment with passive (first order) and active, concentration-dependent transports of RO7049389 into the liver from both the absorption and the plasma compartments and with a first-order elimination of RO7049389 from the liver via the M5 metabolic pathway; (ii) a plasma compartment for RO7049389 with a dose-dependent clearance of RO7049389 via a non-M5 metabolic pathway and potential biliary secretion; (iii) a plasma compartment for metabolite M5 with first-order elimination; and (iv) a transit compartment model to describe the absorption.[7,8] In addition to the concentration-dependent liver uptake contributing to the more-than-dose-proportional increase in RO7049389 exposure, the

dose effect on clearance of RO7049389 from the plasma compartment was included as follows:

$$CL = \theta_{CL} \times \left(\frac{Dose}{200}\right)^{\theta_{Dose}}$$

(θ_{CL} = population estimate of CL (plasma clearance of RO7049389) when dose equals 200 mg; θ_{Dose} = scaling factor quantifying the influence of dose on CL).

Food effect was estimated on the relative bioavailability (rel BA) and on the mean transit time (MTT) according to the following equations:

$$\text{rel BA} = 1 \times \text{Food} + \theta_{Food} \times (1 - \text{Food}).$$

(θ_{Food} = population estimate of BA in fasted relative to fed conditions).

$$MTT = \theta_{MTT} + \theta_{Food} \times \text{Food}$$

(θ_{MTT} = population estimate of MTT in fasted condition; θ_{Food} = scaling factor quantifying the influence of food on MTT).

BSV was incorporated on all parameters except on mass-transfer rate constant between plasma and liver compartments (K32). The RV was found to be adequately accounted for by a combined additive and proportional error model for both RO7049389 and metabolite M5 concentrations, with a correlation between the two proportional parts and the two additive parts of the RV for RO7049389 and M5.

Ethnicity (Asian vs. non-Asian) dependencies were quantified on maximum liver uptake capacity (Vm), CL, plasma volume of RO7049389 (V3) (= plasma volume of M5 (V4)) and the M5-formation rate constant (K_{FM}), and gender effect on CL.

The population PK parameters were precisely estimated (**Table 1**) with relative standard error below 25% for the fixed effect and below 42% for the random effect parameters, and a rather modest eta shrinkage between 2% and 42%. RO7049389 has an increased relative bioavailability of 1 with food vs. 0.439 without food and a slower absorption with a mean transit time of 1.17 hours with food vs. 0.36 hours without food. The plasma clearance of RO7049389 via non-M5 metabolic pathway and potential biliary secretion decreases as dose increases (**Figure 3**). The clearance declines from 72 L/hr at 200 mg to 13 L/hr at 2,500 mg in non-Asian males, and from 33 L/hr at 200 mg to 5.9 L/hr at 2,500 mg in Asian males. The V3, the CL, and the Vm are 38, 54, and 30% lower, respectively, in Asians vs. non-Asians, and the K_{FM} is 62% higher in Asians. Female subjects have a 63% lower CL compared with males. **Figure 4** illustrates the combined effect of ethnicity and gender on the steady-state PK profiles of RO7049389 and M5 after 600 mg q.d. in the fasted condition.

The goodness-of-fit plots presented in **Figure S1 and Figure S2** indicate that both RO7049389 and M5 data are generally well characterized by the PK model considering the complexities of the mechanisms responsible for the nonlinearity and the huge variability in the data. The plot of observations vs. population predictions and vs. individual predictions for RO7049389 display a rather homogeneous distribution around the identity line despite that a number of data points deviate from this distribution with a relative difference between observation and population prediction larger than 40%. Those points, identified in 11 individuals, belong to the absorption period. Indeed, there is a shift between individual observed and the population predicted time to reach maximum plasma concentration. This heterogeneity in the absorption profiles being more prominent in RO7049389 than in M5 is believed to be mainly responsible for the large residual variability for RO7049389, 45%, as compared with the 23% for M5. Also, regarding the plots, it can be noticed a tendency towards lower population predictions than observations for predictions below 0.5 ng/mL; this artificial bias is likely due to the fact that during absorption delay or at the latest time only concentrations above the limit of quantification (of 1 ng/mL) can be observed. The plots of conditional weighted residuals vs. time or vs. population prediction for RO7049389 showed a random distribution of data points around the zero line, with the majority of data within two times the SDs. The inspection of the goodness-of-fit plots for M5 leads to similar conclusions as for RO7049389. The results of the visual predictive check showed that the median of the observed RO7049389 and M5 profiles were contained in their respective 90% confidence intervals (**Figure S3 and Figure S4**). It indicated that the structure of the model was adequate to describe the PK behavior across doses, regimens, and ethnic groups. The 5th and 95th percentiles of the observed RO7049389 and M5 profiles were frequently outside the confidence interval; the model had the tendency to overestimate the variances.

Simulation results

Deriving and summarizing the individual exposure parameters by dose and ethnic group from the simulated time courses (**Table 2**), the combined effects of ethnicity on the PK parameters lead to C_{max} and AUC of RO7049389 in plasma 1.9 to 2.3 times higher in Asians than in non-Asians, while A_{max} and AUQ in the liver are comparable between the two ethnic groups with a ratio of exposure in Asians vs. non-Asians from 0.7 to 0.9. For M5, the effects of ethnicity lead to C_{max} and AUC in plasma 1.2 to 1.6 times higher in Asians. Noticeably, the interindividual variability in A_{max} and AUQ is reduced in the liver (32–38% and 64–94%, respectively) compared with plasma C_{max} and AUC (71–141%, and 102–113%, respectively).

The gender effect on plasma clearance leads to C_{max} and AUC of RO7049389 in plasma 1.8 to 2.1 and 2.1 to 2.6 times higher in females, respectively (across doses and ethnic groups). It leads to similar A_{max} of RO7049389 in the liver between females and males and to AUQ in the liver that are 1.2 to 1.5 times higher in females. C_{max} and AUC of M5 in plasma are 1.2 to 1.4 and 1.3 to 1.6 times higher in females, respectively.

The comparison of the steady-state PK profiles with the 90% prediction interval between Asian and non-Asian subjects is shown for the dose of 600 mg q.d., fasted condition, in **Figure 5a** for RO7049389 in plasma and in the liver and **Figure 5b** for M5 in plasma.

DISCUSSION

Across all phases of drug development, it is essential to understand how the concentration of a drug changes within subject populations treated with clinically relevant doses. PopPK enables identification of the sources of between-individual and within-individual variability in drug concentrations in cohorts of healthy volunteers and HBV patients, and accounts for the variability in terms of patient characteristics such as age, ethnicity, gender, or disease state. PopPK is frequently used to drive

Table 1 Model parameter estimates

Parameters	Estimate	RSE (%)	95% CI[a]	CV	Shrinkage (%)
Fixed effect parameters					
θ_1 Vm[b] (mMol/h)	0.123	12.1	(0.0499, 0.232)	–	–
θ_2 Km[b] (mMol)	0.00107	13.1	(0.000585, 0.00151)	–	–
θ_3 CL (L/h)	71.7	13.9	(51.4, 96.1)	–	–
θ_4 V3 (=V4) (L)	10.2	9.19	(7.36, 12.4)	–	–
θ_5 K23 (1/h)	1.18	5.68	(0.799, 1.45)	–	–
θ_{18} K32 (1/h)	0.377	18.1	(0.0413, 0.687)	–	–
θ_6 K_{FM} (1/h)	0.0318	9.94	(0.0159, 0.04)	–	–
θ_7 CL_M (L/h)	1.27	7.60	(0.708, 1.87)	–	–
θ_{10} Ka (1/h)	1.03	11.7	(0.831, 2.2)	–	–
θ_{11} MTT (h)	0.360	8.08	(0.252, 0.608)	–	–
θ_{12} N	7.24	15.2	(4.09, 9.87)	–	–
Dose effect parameter					
θ_9 Dose (mg) on CL	−0.684	8.35	(−0.839, −0.417)	–	–
Food effect parameters					
θ_8 rel BA in fasted state	0.439	2.42	(0.366, 0.539)	–	–
θ_{13} Food on MTT (h)	0.805	7.45	(0.389, 1.11)	–	–
Asian effect parameters					
θ_{14} Asian on Vm	0.699	20.0	(0.524, 1.12)	–	–
θ_{15} Asian on CL	0.460	20.0	(0.326, 0.6)	–	–
θ_{16} Asian on V3	0.619	13.7	(0.47, 0.734)	–	–
θ_{17} Asian on K_{FM}	1.62	16.5	(1.21, 2.28)	–	–
Gender effect parameter					
θ_{19} Gender on CL	0.369	24.1	(0.257, 0.562)	–	–
Random effect parameters (BSV)					
ω_1^2 on Vm	0.402	24.3	(0.271, 0.861)	63.4%	19.2
ω_2^2 on Km	0.670	19.7	(0.0466, 1.10)	81.9%	18.2
ω_3^2 on CL	0.542	14.4	(0.294, 0.740)	73.6%	1.70
ω_4^2 on V3	0.0853	33.2	(0.0335, 0.195)	29.2%	36.8
ω_5^2 on K_{FM}	0.180	34.6	(0.0887, 0.257)	42.4%	28.1
ω_6^2 on CL_M	0.113	29.5	(0.0323, 0.257)	33.6%	40.8
ω_7^2 on Ka	0.277	41.5	(0.0544, 0.78)	52.6%	41.7
ω_8^2 on MTT	0.277	16.7	(0.134, 0.422)	52.6%	9.17
ω_9^2 on N	0.862	22.3	(0.148, 1.57)	92.8%	26.6
ω_{10}^2 on K23	0.143	21.5	(0.00678, 0.230)	37.8%	18.3
Random effect parameters (RV)					
σ_1^2 Prop. RV for RO7049389	0.205	3.05	(0.183, 0.235)	45.3%	
σ_2^2 Prop. RV for M5	0.0523	2.50	(0.0418, 0.0676)	22.8%	
σ_{1-2} Cov. between σ_1 and σ_2	0.0418	5.77	(0.0302, 0.0501)	0.404[c]	
σ_3^2 Add. RV for RO7049389	3.74	12.4	(0.982, 7.32)	1.93 ng/mL[d]	
σ_4^2 Add. RV for M5	457	13.2	(15.4, 1190)	21.4 ng/mL[d]	
σ_{3-4} Cov. between σ_3 and σ_4	34.8	13.0	(4.41, 80.3)	0.843[c]	

Add., additive; BSV, between-subject variability; CI, confidence interval; CL, plasma clearance of RO7049389; CL_M, clearance of M5; Cov., covariance; CV, coefficient of variation; h, hour; Ka, the absorption rate constant (first order process); K_{FM}, M5-formation rate constant (first-order process); Km, Michaelis-Menten constant of the liver uptake capacity; K23, mass-transfer rate constant between plasma and liver compartments (first order process); K32, mass-transfer rate constant between liver and plasma compartments (first order process); MTT, mean transit time; N, number of transit compartments; Prop., proportional; rel BA, relative bioavailability; RSE, relative standard error of estimate; RV, residual variability Vm, maximum liver uptake capacity; V3, plasma volume of RO7049389; —, not applicable.
[a]Calculated using bootstrap procedure. [b]The molecular weight of RO7049389 is 598.69 g/mol. [c]Correlation. [d]Reported as standard deviation.

decision making related to optimal drug dosing in subpopulations,[9,10] to inform recommendations on therapeutic individualization (e.g., personalized dosing), and to provide essential support for efficacy and safety in marketing applications of new molecular entities.

The pharmacokinetics (PK) of RO7049389, a new HBV core protein allosteric modulator of class I, and of its active metabolite M5 were studied in fasted and fed conditions after single and multiple once-a-day and twice-a-day doses in healthy subjects and HBV patients. A popPK model, simultaneously modeling RO7049389 and its active metabolite M5, was developed to infer the quantity of RO7049389 in the liver relative to plasma and to quantify the ethnicity (i.e., Asian vs. non-Asian) and gender effects on the PK of RO7049389 and M5. Exposures in the liver are of particular importance for dose selection since the liver is the site of action of the compound. The evaluation of the model generally confirmed its ability to adequately describe the observed measurements.

RO7049389 is a molecule with physicochemical and pharmacokinetic properties that make it suitable to reach its site of action in the liver and was characterized as showing strong antiviral activity in preclinical models of HBV. Specifically, RO7049389 was selected for clinical development as a substrate of human liver uptake transporters (OATP1B1 and OATP1B3). This leads to intracellular accumulation in incubations with hepatocytes since the OATP influx transporters are expressed on the basolateral membrane of hepatocytes and serve to increase intrahepatic concentrations relative to plasma. In contrast, the active metabolite M5 has a higher passive permeability and is not a substrate of OATPs. RO7049389 has moderate passive permeability and is a substrate of human Pgp but not of BCRP. Its elimination appears to be mainly mediated by liver metabolism. These molecular properties informed the construction of the PopPK model described here. To account for these specific properties, the structure of the PK model was built around a disposition compartment representing the liver connected to an absorption compartment representing the gut and to a second disposition compartment representing the plasma. The active uptake into the liver from the gut and from the plasma was described using the same concentration-dependent (i.e., Michaelis-Menten) equation. In parallel to this active uptake, RO7049389 could be passively absorbed from the gut via a first-order process and could passively distribute back and forth from the liver to the plasma compartment via first-order processes. The elimination of RO7049389 occurred via the liver to form metabolite M5 and via the plasma compartment, representing the non-M5 metabolic pathway and potential biliary secretion, through dose-dependent first-order process. A model considering only an elimination via the liver with two parallel processes, one representing the M5 metabolic pathway and the other one the non-M5 metabolic pathway, was tested; however, this approach was not able to describe accurately the PK of RO7049389 in plasma. To describe the slow absorption of RO7049389 a chain of transit compartments was used before the absorption compartment.[7,8] An active efflux from the liver back to the gut that would impact the absorption process was not considered because of the saturation of that process at the administered doses. Remarkably, the processes governing the PK of metabolite M5 were all found to be linear, indicating that the observed less-than-dose-proportional increase in M5 exposure could be fully attributed to the nonlinear PK of RO7049389. Furthermore, model-estimated unbound liver concentrations across the full dose range were below the measured *in vitro* Michaelis-Menten constant for CYP3A-mediated metabolism to M5 of 20 μM, indicating that saturation of hepatic metabolism is

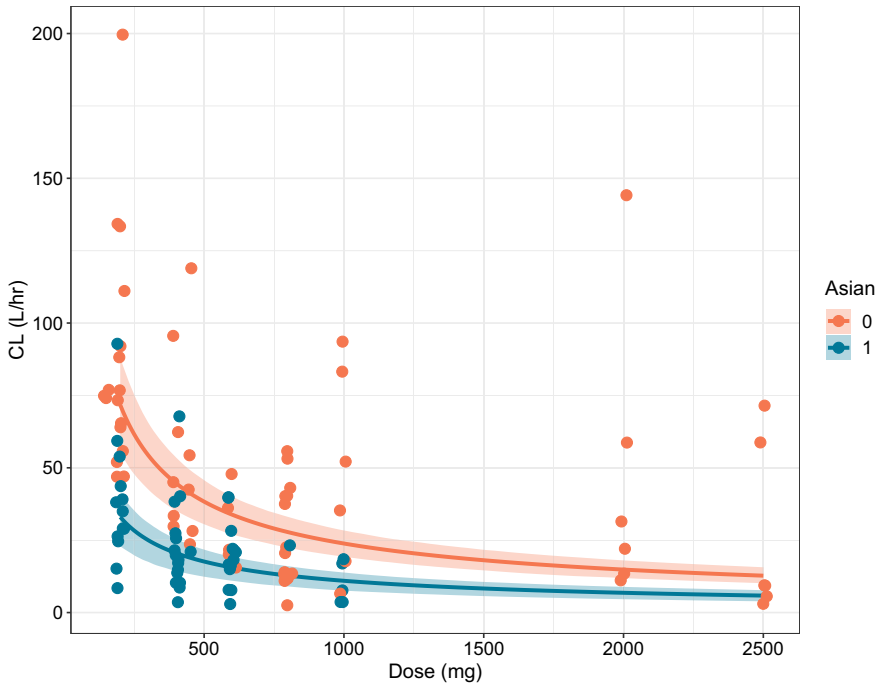

Figure 3 Dose effect on plasma clearance of RO7049389 in males. The thick lines represent the population relationship between CL and dose for male non-Asians and Asians; the symbols are the individual predicted CL values. CL, plasma clearance of RO7049389.

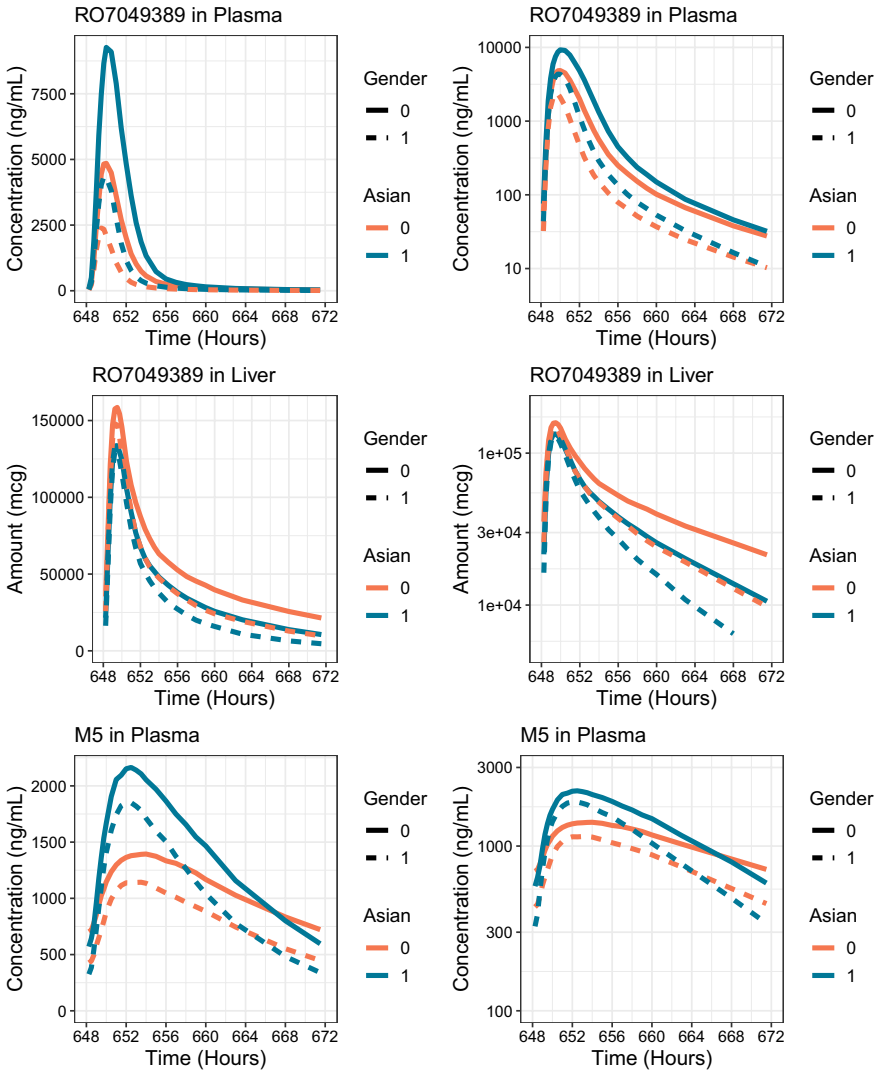

Figure 4 Effect of gender and ethnicity on the steady-state PK profiles of RO7049389 and M5 at 600 mg q.d. fasted. Left column, linear Y scale. Right column, logarithmic Y scale. PK, pharmacokinetic; q.d., once a day.

unlikely. However, we accept that the uncertainties in estimation of hepatic free concentration combined with the uncertainty in *in vitro* measurement and translation to *in vivo* mean that saturation of hepatic metabolism cannot be excluded.

Although this model structure incorporates mechanistic knowledge gained from preclinical development and physiologically-based PK modeling, it cannot be considered fully mechanistic. Indeed, few simplifications were necessary to comply with the parsimony principle of a data-driven model development. The multiplicity of the processes governing the elimination and the metabolism of RO7049389 (i.e., passive transport, active uptake by the liver, active efflux from the liver, potential saturable metabolism by CYP 3A4 and UGT 1A3, potential biliary secretion, and their interplay) could not be fully captured with only RO7049389 and M5 plasma concentrations. One of the simplifications was to use apparent dose dependencies and ethnicity dependencies on the plasma clearance for RO7049389 (**Figure 3**) to represent its non-M5 metabolic pathway that should have occurred normally in the liver compartment after active uptake but also its potential biliary secretion suspected on the basis of detection of RO7049389 in the bile of bile duct-cannulated rats. The use of more mechanistic equations with concentration dependency instead of dose dependency was attempted but proved unsuccessful. Beside those simplifications, the model demonstrated to be robust enough to assess covariate effects and to run simulation.

The population analysis revealed also large unexplained BSV (i.e., above 50%) on numerous PK parameters describing absorption, metabolism, and elimination of RO7049389. This overall large variability observed in the PK can be partially attributed to the genetic variability in genes encoding OATP transporters. It has been shown that a single nucleotide polymorphism in the SLCO1B1 gene encoding OATP1B1 decreases the ability of OATP1B1 to transport active simvastatin acid from portal circulation into the liver, resulting in markedly increased plasma concentrations of simvastatin acid.[11] Large variability in exposure is reported for many other OATP1B1 substrate drugs.[12]

Table 2 Plasma and liver RO7049389 exposure and plasma M5 exposure

Dose	Exposure parameter	Non-Asian	Asian	Geometric mean ratio Asian/ Non-Asian (90% CI)
Plasma RO7049389				
200 mg	C_{max} (ng/mL)	396 (141%)	915 (139%)	2.31 (2.14–2.49)
	AUC (ng·h/mL)	1,353 (104%)	2,794 (113%)	2.07 (1.94–2.20)
400 mg	C_{max} (ng/mL)	1,607 (112%)	3,617 (88.4%)	2.25 (2.12–2.39)
	AUC (ng·h/mL)	4,654 (111%)	10,429 (106%)	2.24 (2.10–2.39)
600 mg	C_{max} (ng/mL)	3,614 (86.5%)	6,828 (81.3%)	1.89 (1.79–1.99)
	AUC (ng·h/mL)	10,732 (107%)	21,334 (107%)	1.99 (1.86–2.12)
1,000 mg	C_{max} (ng/mL)	7,706 (71.3%)	15,132 (69.6%)	1.96 (1.87–2.06)
	AUC (ng·h/mL)	25,200 (102%)	55,089 (104%)	2.19 (2.05–2.33)
Liver RO7049389*				
200 mg	A_{max} (mg)	75.8 (31.7%)	64.5 (32.6%)	0.85 (0.83–0.87)
	AUQ (mg·h)	530 (93.5%)	385 (87.7%)	0.73 (0.69–0.77)
400 mg	A_{max} (mg)	125 (37.9%)	106 (35.7%)	0.85 (0.84–0.88)
	AUQ (mg·h)	840 (90.2%)	636 (77.8%)	0.76 (0.72–0.79)
600 mg	A_{max} (mg)	162 (34.6%)	139 (34.4%)	0.86 (0.84–0.88)
	AUQ (mg·h)	1,060 (75.3%)	803 (70.8%)	0.76 (0.72–0.79)
1,000 mg	A_{max} (mg)	230 (36.4%)	208 (32.2%)	0.90 (0.88–0.93)
	AUQ (mg·h)	1,436 (74.6%)	1,180 (64.3%)	0.82 (0.78–0.86)
Plasma M5				
200 mg	C_{max} (ng/mL)	633 (91.4%)	935 (78.0%)	1.48 (1.40–1.56)
	AUC (mcg·h/mL)	10.9 (117%)	13.0 (109%)	1.19 (1.12–1.27)
400 mg	C_{max} (ng/mL)	998 (93.2%)	1,530 (72.8%)	1.53 (1.45–1.62)
	AUC (mcg·h/mL)	17.3 (117%)	21.7 (96.7%)	1.25 (1.18–1.34)
600 mg	C_{max} (ng/mL)	1,287 (81.8%)	2,011 (68.4%)	1.56 (1.49–1.64)
	AUC (mcg·h/mL)	22.1 (102%)	27.6 (92.8%)	1.25 (1.18–1.33)
1,000 mg	C_{max} (ng/mL)	1,835 (76.2%)	2,990 (65.6%)	1.63 (1.55–1.71)
	AUC (mcg·h/mL)	30.5 (96.5%)	40.2 (87.2%)	1.32 (1.24–1.40)

AUC, area under the plasma concentration profile; A_{max}, maximum liver amount; AUQ, area under the liver amount profile; C_{max}, maximum plasma concentration. Plasma and liver RO7049389 exposure and plasma M5 exposure (geometric mean (geometric %CV)) by ethnic groups (q.d. fasted regimen).
*[Correction added on 24 March 2021, after first online publication: The units of A_{max} and AUQ in liver has been corrected to (mg) and (mg·h) from (mcg) and (mcg/h).]

The covariate effects investigation indicated that the Vm is reduced in Asians while the K_{FM} is increased. In a review of the ethnic variability in the plasma exposure of OATP1B1 substrates such as statins, Tomita *et al*. have demonstrated that large variability alone cannot explain the large difference in plasma exposure between Asians and non-Asians and that the OATP1B1-mediated hepatic uptake activity depends also on race with a lower OATP1B1 activity or protein expression in Asians.[12] Several OATP1B1-substrate drugs show larger AUC levels in plasma in Asians than in White patients. Interestingly, simulations using a PBPK model for pravastatin showed that the change in hepatic uptake activity greatly affects the plasma exposure but not the hepatic exposure.[13,14] The increase of K_{FM} in Asians can be related to higher expression levels of adult liver CYP3A4 messenger RNAs in Japanese vs. White patients and higher clearance of midazolam, a CYP3A4 substrate, observed in healthy age-matched males of South Asian compared with White ancestry that was not explained by differences in the frequency of CYP3A genotypes.[15,16] The V3 and CL were also found to be smaller in Asians. Those effects can be considered apparent, i.e., to be the consequence of the simplification of the model. The lower V3 in Asians is probably not due to a difference in plasma protein binding between ethnic groups, since albumin is the main plasma binding protein for RO7049389. A correlation between ethnicity effect on volume and weight cannot be ruled out, as Asians are overall slightly lighter than non-Asians.

The apparent total clearance of RO7049389 was found to be reduced in females. The reason for this gender effect is not known. One explanation may be that this effect is due to a gender difference in the OATP1B1-mediated hepatic uptake as shown in a PK study of torsemide, a substrate of OATP1B1, in which gender was identified as a potential determinant of greater exposure in females beyond the SLCO1B1 single nucleotide polymorphism.[17] Although there are, to date, few reports on clinical effect of gender on OATP activity, it has been shown that liver transport proteins of the OATP family are expressed and regulated in a gender-specific manner in rats.[18] The known gender effect on CYP3A4,[19] the major metabolic pathway of RO7049389, does not appear to be a potential reason for the observed difference because it should

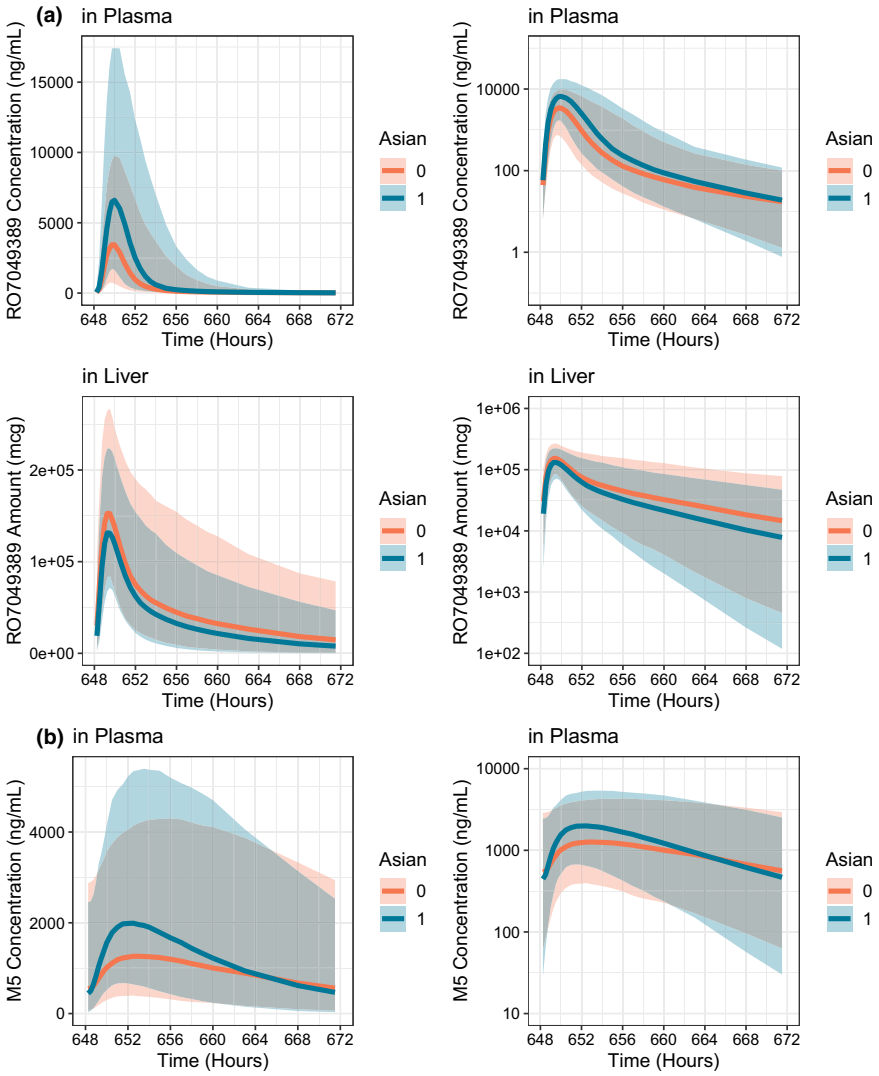

Figure 5 Comparison of steady-state plasma and liver PK profiles of (**a**) RO7049389 and plasma PK profiles of (**b**) M5 at 600 mg q.d. fasted between Asian and non-Asian subjects. Bold line, median of 1,000 simulated profiles; shaded area, 90% prediction interval. Left column of each panel, linear Y scale. Right column of each panel, logarithmic Y scale. PK, pharmacokinetic; q.d., once a day.

have led to a lower plasmatic exposure as the activity of CYP3A4 is higher in females.

Food was found to delay slightly the absorption and approximately double the bioavailability. These effects can be linked respectively to slower gastric emptying and to the low solubility of RO7049389, which is higher (Roche data on file) in the presence of intraluminal bile salts released when a meal is consumed.

Once the covariate effects were accounted for, the PK of RO7049389 and of metabolite M5 were found to be similar between healthy subjects and HBV patients. No additional covariate dependencies with weight and age were identified on the PK parameters.

Interestingly, the observed effect on HBV DNA was similar between Asians and non-Asians. In addition, the exposure–response analysis using a viral kinetic model showed that it is the liver exposure and not the plasma exposure best driving the HBV DNA decline, with similar relationship between Asian and non-Asian patients with chronic HBV infection.[20] We acknowledge that the high effectiveness (i.e., drug effect on the virus production) of RO7049389[20] at low dose (200 mg q.d., fasted condition) makes it difficult to definitely determine which specific exposure between liver and plasma leads to the best exposure–response relationship. However, small changes in effectiveness percentage can lead to more substantial change in the log drop of the HBV DNA (the efficacy end point).[21] As the liver is the target organ for the antiviral action of RO7049389 and the efficacy is coming mainly from the parent drug, the results of the population PK modeling and the exposure–response analysis, associated with a favorable safety profile, support the selection of the same therapeutic dose of RO7049389 for patients with different ethnicity.

As mentioned above, research on compounds sharing the same molecular properties as RO7049389 has shown larger AUC levels in plasma in Asians than in White patients likely due to a lower OATP1B1 activity or protein expression in Asians, and simulations using a PBPK model have demonstrated that the change in

hepatic uptake activity greatly affects the plasma exposure but not the hepatic exposure. This work provides additional insight by quantifying the exposure and estimating the sources of variability in the site of action for OATP1B1-substrate drugs.

SUPPORTING INFORMATION

Supplementary information accompanies this paper on the *Clinical Pharmacology & Therapeutics* website (www.cpt-journal.com).

ACKNOWLEDGMENTS

The authors thank all the participants in the trials from which data were derived for purposes of the analyses. Hoffmann-La Roche, Ltd. sponsored all of the trials. The authors also thank Giulio Fiaschetti for editorial assistance.

FUNDING

Funding for all clinical trials referenced was provided by Hoffmann-La Roche, Ltd.

CONFLICT OF INTEREST

All authors are current employees of Hoffmann-La Roche and own shares of the company.

AUTHOR CONTRIBUTIONS

V.C., S.F., A.L.-D., and N.P. wrote the manuscript. S.F., Q.B., and Y.J. designed the research. V.C. performed the research. V.C., S.F., F.J., A.L.-D., A.P., N.P., and Y.J. analyzed the data.

1. EASL. 2017 Clinical Practice Guidelines on the management of hepatitis B virus infection. *J. Hepatol.* **67**, 370–398 (2017).
2. World Health Organization. Hepatitis B fact sheet <https://www.who.int/en/news-room/fact-sheets/detail/hepatitis-b> (July 27, 2020). Accessed September 2020.
3. Fernández, M., Quiroga, J.A. & Carreño, V. Hepatitis B virus downregulates the human interferon-inducible MxA promoter through direct interaction of precore/core proteins. *J. Gen. Virol.* **84**, 2073–2082 (2003).
4. Gruffaz, M. *et al*. Hepatitis B core (HBC) protein is a key and very early negative regulator of the interferon response [Poster Abstract 378]. *J. Hepatol.* **58**, S155–156 (2013).
5. Twu, J.S., Lee, C.H., Lin, P.M. & Schloemer, R.H. Hepatitis B virus suppresses expression of human beta-interferon. *Proc. Natl. Acad. Sci. U S A* **85**, 252–256 (1988).
6. Feng, S. *et al*. A five-in-one first-in-human study to assess safety, tolerability, and pharmacokinetics of RO7049389, an inhibitor of hepatitis B virus capsid assembly, after single and multiple ascending doses in healthy participants. *Antimicrob. Agents Chemother.* 64, e01323-20 (2020).
7. Savic, R.M., Jonker, D.M., Kerbusch, T. & Karlsson, M.O. Implementation of a transit compartment model for describing drug absorption in pharmacokinetic studies. *J. Pharmacokinet. Pharmacodyn.* **34**, 711–726 (2007).
8. Wilkins, J.J. *et al*. Population pharmacokinetics of rifampin in pulmonary tuberculosis patients, including a semimechanistic model to describe variable absorption. *Antimicrob. Agents Chemother.* **52**, 2138–2148 (2008).
9. Lee, J.Y. *et al*. Impact of pharmacometric analyses on new drug approval and labelling decisions: a review of 198 submissions between 2000 and 2008. *Clin. Pharmacokinet.* **50**, 627–635 (2011).
10. Marshall, S.F. *et al*. Good practices in model-informed drug discovery and development: practice, application, and documentation. *CPT Pharmacometrics Syst. Pharmacol.* **5**, 93–122 (2016).
11. Kalliokoski, A. & Niemi, M. Impact of OATP transporters on pharmacokinetics. *Brit. J. Pharmacol.* **158**, 693–705 (2009).
12. Tomita, Y., Maeda, K. & Sugiyama, Y. Ethnic variability in the plasma exposures of OATP1B1 substrates such as HMG-CoA reductase inhibitors: a kinetic consideration of its mechanism. *Clin. Pharmacol. Ther.* **94**, 37–51 (2013).
13. Watanabe, T. *et al*. Investigation of the rate-determining process in the hepatic elimination of HMG-CoA reductase inhibitors in rats and humans. *Drug Metab. Dispos.* **38**, 215–222 (2010).
14. Watanabe, T., Kusuhara, H. & Sugiyama, Y. Application of physiologically based pharmacokinetic modeling and clearance concept to drugs showing transporter-mediated distribution and clearance in humans. *J. Pharmacokinet. Pharmacodyn.* **37**, 575–590 (2010).
15. Yamaori, S. *et al*. Ethnic differences between Japanese and Caucasians in the expression levels of mRNAs for CYP3A4, CYP3A5, and CYP3A7. *Xenobiotica* **35**, 69–83 (2005).
16. van Dyk, M., Marshall, J.-C., Sorich, M.J., Wood, L.S. & Rowland, A. Assessment of inter-racial variability in CYP3A4 activity and inducibility among healthy adult males of Caucasian and South Asian ancestries. *Eur. J. Clin. Pharmacol.* **74**, 913–920 (2018).
17. Werner, U. *et al*. Gender is an important determinant of the disposition of the loop diuretic torasemide. *J. Clin. Pharmacol.* **50**, 160–168 (2010).
18. Rost, D. *et al*. Gender-specific expression of liver organic anion transporters in rat. *Eur. J. Clin. Invest.* **35**, 635–643 (2005).
19. Tanaka, E. Gender-related differences in pharmacokinetics and their clinical significance. *J. Clin. Pharm. Ther.* **24**, 339–346 (1999).
20. Gonçalves, A. *et al*. What drives the dynamics of HBV RNA during treatment? *J. Viral Hepat.* 28, 383–392 (2021).
21. Perelson, A.S. & Guedj, J. Modelling hepatitis C therapy—predicting effects of treatment. *J. Nat. Rev. Gastroenterol. Hepatol.* **12**, 437–445 (2015).